Science of the Total Environment 927 (2024) 172003

Contents lists available at ScienceDirect

Science of the Total Environment

journal homepage: www.elsevier.com/locate/scitotenv

Heavy metal induced shifts in microbial community composition and interactions with dissolved organic matter in coastal sediments

Yu Wang [a,b,1], Yuxing Hu [a,1], Yanting Liu [a], Qi Chen [a], Jinxin Xu [a], Fei Zhang [c], Jinhua Mao [a], Quan Shi [d], Chen He [d], Ruanhong Cai [a], Christian Lønborg [e], Lihua Liu [f], Aixing Guo [a], Nianzhi Jiao [a,*], Qiang Zheng [a,*]

[a] State Key Laboratory of Marine Environmental Science, College of Ocean and Earth Science, Xiamen University, Xiamen, China
[b] College of Environmental and Ecology, Xiamen University, Xiamen, China
[c] Third Institute of Oceanography Ministry of Natural Resources, Xiamen, China
[d] College of Chemical Engineering and Environment, China University of Petroleum (Beijing), Beijing, China
[e] Department of Ecoscience, Section for Marine Diversity and Experimental Ecology, University of Aarhus, Roskilde, Denmark
[f] Fujian Xiamen Environmental Monitoring Central Station, Xiamen, China

HIGHLIGHTS

- Heavy metals change the dissolved organic matter composition.
- Contributions of recalcitrant organic matter increases when heavy metals are present.
- Archaeal communities are more negatively impacted by heavy metals than bacteria.
- Microbial interactions with organic matter shift under heavy metal stress.

GRAPHICAL ABSTRACT

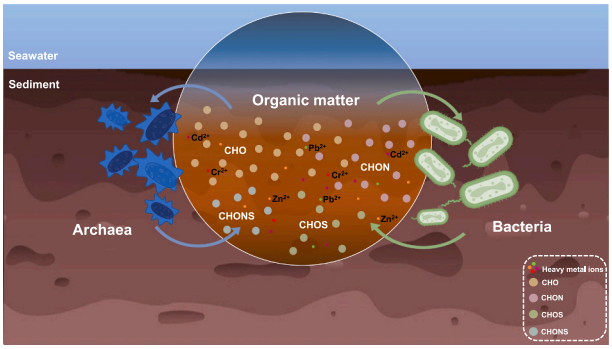

ARTICLE INFO

Editor: Christopher Rensing

Keywords:
Heavy metal pollution
Dissolved organic matter
Microbial community
Sediment
Organic matter chemical composition

ABSTRACT

Heavy metals can impact the structure and function of coastal sediment. The dissolved organic matter (DOM) pool plays an important role in determining both the heavy metal toxicity and microbial community composition in coastal sediments. However, how heavy metals affect the interactions between microbial communities and DOM remains unclear. Here, we investigated the influence of heavy metals on the microbial community structure (including bacteria and archaea) and DOM composition in surface sediments of Beibu Gulf, China. Our results revealed firstly that chromium, zinc, cadmium, and lead were the heavy metals contributing to pollution in our studied area. Furthermore, the DOM chemical composition was distinctly different in the contaminated area from the uncontaminated area, characterized by a higher average O/C ratio and increased prevalence of carboxyl-rich alicyclic molecules (CRAM) and highly unsaturated compounds (HUC). This indicates that DOM in the contaminated area was more recalcitrant compared to the uncontaminated area. Except for differences in

* Corresponding authors.
E-mail addresses: jiao@xmu.edu.cn (N. Jiao), zhengqiang@xmu.edu.cn (Q. Zheng).
[1] Yu Wang and Yuxing Hu contribute equally.

https://doi.org/10.1016/j.scitotenv.2024.172003
Received 6 February 2024; Received in revised form 23 March 2024; Accepted 25 March 2024
Available online 2 April 2024

archaeal diversity between the two areas, there were no significant variations observed in the structure of archaea and bacteria, as well as the diversity of bacteria, across the two areas. Nevertheless, our co-occurrence network analysis revealed that the B2M28 and Euryarchaeota, dominating bacterial and archaeal groups in the contaminated area were strongly related to CRAM. The network analysis also unveiled correlations between active bacteria and elevated proportions of nitrogen-containing DOM molecules. In contrast, the archaea-DOM network exhibited strong associations with nitrogen- and sulfur-containing molecules. Collectively, these findings suggest that heavy metals indeed influence the interaction between microbial communities and DOM, potentially affecting the accumulation of recalcitrant compounds in coastal sediments.

1. Introduction

Globally, many coastal sediments contain potentially harmful pollutants originating from diverse human activities (Chen et al., 2018; Superville et al., 2014). Among these pollutants, heavy metals are particularly concerning as they act as biotoxins, persist in the environment, and have the capacity to bioaccumulate (Chen et al., 2018; Chen et al., 2004; Dou et al., 2013). Numerous studies have demonstrated that, for instance, high levels of heavy metals such as cadmium (Cd), mercury (Hg), copper (Cu), and zinc (Zn) can impact the health and function of many marine organisms (Liu et al., 2017).

Sediment prokaryotes, including bacteria and archaea, play key roles in the biogeochemical cycling of carbon, nitrogen, and other elements (Parkes et al., 2014). Prokaryotes also have a substantial influence on the fate of contaminants (Ford et al., 1998), with bacteria, in particular, serving as the initial link in transferring toxic compounds to higher trophic levels (Gillan et al., 2005). In contrary, heavy metals also exhibit strong influences on the diversity and structure of the prokaryotic community (He et al., 2019), with heavy metal toxicity being a significant driver of microbial community changes. Microorganisms have different sensitivities to heavy metals (Rajeev et al., 2021), potentially leading to the replacement of sensitive ones by heavy metal-tolerant microbes in contaminated areas (Tipayno et al., 2018). Previous studies have revealed how heavy metal pollution enhances the proportions of Actinobacteria, Bacteroidetes, Deinococcus-Thermus, and Chloroflexi while decreasing the abundances of Proteobacteria and Acidobacteria (Zeng et al., 2020). Thus, heavy metal pollution may have significant implications for microbial communities in coastal sediments (Dell'Anno et al., 2003). Additionally, microorganisms are also recognized as potential pollution indicators as they reflect the overall pollution status through changes in abundance, taxonomic composition, functional capabilities, and the presence or absence of specific indicator species (Song et al., 2016; Tang et al., 2019). Here it is important to remember that a large fraction of heavy metals in sediments are strongly absorbed by organic matter present, with these organics influencing the toxicity, fate, and bioavailability of the metals (Pontoni et al., 2022). In these interactions especially the dissolved organic matter (DOM) pool is thought to be important in structuring the prokaryotes community and it constitutes a large fraction of the organic molecules interacting with heavy metals (Li et al., 2021; Zeng et al., 2024). Consequently, due to the growing impact of human-induced pollution on microbial populations, it is essential to investigate the interactions between microorganisms, heavy metals, and organic matter to accurately understand pollution impacts and feedbacks in coastal sediments.

The Beibu Gulf, situated in the northwestern region of the South China Sea, has over the past few decades witnessed large economic development and urban expansion in the coastal cities surrounding its northern shores. This development has increased inputs of heavy metals and other pollutants (Chen et al., 2018; Liu et al., 2020), with previous studies suggesting that these increased inputs could negatively impact organisms spanning from microbes to humans (Liu et al., 2020). Heavy metals are transported into coastal waters from natural and anthropogenic sources, including from river runoff, atmospheric deposition, and industrial and agricultural activities (Wu et al., 2017; Zheng et al., 2008). Here heavy metals from natural sources are typically unavailable to organisms, while those from anthropogenic sources are bioavailable (Davis et al., 2003). In this study, we examined the potential interaction between microbial communities, DOM, and heavy metals in surface sediment along the northern coast of the Beibu Gulf, by combing high-throughput sequencing and high-resolution mass spectra technologies. We aimed to answer the following questions: 1) how are prokaryote (bacterial and archaeal) diversity and structure impacted by heavy metals? 2) do heavy metals influence the DOM properties? and 3) do interactions between microbial communities and the DOM pool change with increasing heavy metal levels? Our analyses offer valuable insights into how heavy metal pollution impacts the composition of sedimental microbial communities and the interactions between microbes and DOM.

2. Methods and materials

2.1. Sampling sites and surface sediment collection

In the Beibu Gulf, several rivers from the southern regions of Guangxi, the southwest of Guangdong, and western Hainan Island deliver industrial, agricultural, and urban domestic wastewater into the eastern parts of the Gulf (Gu et al., 2018; Xu et al., 2019). In addition, shipping and tourism activities contribute to heavy metal pollution in the Beibu Gulf (Brtnicky et al., 2020; Chan et al., 2001), with several ports (e.g., Wushi port and Haikou port) and tourist islands (e.g., Weizhou Island and Xieyang Island) serving as potential pollution sources. Sediments in the Beibu Gulf play a pivotal role in the geochemical dynamics of heavy metals, acting simultaneously as sinks and potential sources of these contaminants (Wang et al., 2015; Yu et al., 2008), underscoring their importance in environmental assessments within this marine ecosystem.

In this study three sections were selected in the northeastern part of Beibu Gulf, labeled as section 1 (S01-S04), section 2 (S08-10), and section 3 (S11 and S14-17), with water depths ranging from 5 to 10 m (Fig. 1 and Table S1). These three sections cover the coastal area of Beihai City, several ports, Weizhou Island, and Xieyang Island, which all could be possible sources of anthropogenic heavy metals. A mud sampler was used to collect surface sediments (0–10 cm), with impurities such as sand and gravel being removed before further processing of the samples. Approximately 50 to 100 g of surface sediments were collected in a 50 mL centrifuge tube during March 29–31, 2019 (Fig. 1). The samples were stored at low temperatures and returned to the laboratory within 4 h. Subsequently, the sediment samples were stored at −20 °C until further processing.

2.2. Heavy metal measurement and risk influence evaluation

Sediment samples were dried at 80–100 °C, grounded to a grain size and passed through a 200-mesh, and stored in a 50 mL centrifuge tube at room temperature until further processing (1 month later). For heavy metal analysis, acid digestion of the powdered sample (0.25 g) was performed in a Teflon bomb with an acid mixture (HNO_3-HCl-HF) (Loring and Rantala, 1992) before heating to 120 °C for 12 h on a heating plate. The concentrations of the heavy metals lead (Pb) and cadmium (Cd) were analyzed using graphite furnace atomic absorption

spectrophotometry, while the concentrations of the heavy metals copper (Cu), chromium (Cr), and zinc (Zn) were analyzed using flame atomic absorption spectrophotometry. Arsenic (As) concentration was measured using the hydride generation-atomic fluorescence spectrometry method. Mercury (Hg) was dissolved using a mixture of HNO_3 + H_2SO_4 + V_2O_5, and its concentration was analyzed using cold vapor atomic fluorescence spectrometry. The instruments employed for the analysis of Cd, Cr, Cu, Zn, and Pb were the 220FS 200Z model atomic absorption spectrophotometer, while the HG-AFS atomic fluorescence spectrometer was used for the analysis of Hg and As. Blanks and Chinese standard reference materials (GSS1, GSS2, GSD9, GSD10, and GBW07313) were included in the analyses for data quality monitoring. These results demonstrated that the relative standard deviation was <10 for the heavy metal elements.

To evaluate the potential influence of heavy metals on the sediments, a potential ecological risk index (*RI*), which can quantitatively indicate the degree of pollution and potential ecological risk caused by single or multiple pollutants, was calculated following the method proposed by Hakanson (1980):

$$C_f^i = \frac{C^i}{C_n^r} \quad (1)$$

$$E_r^i = T_r^i \times C_f^i \quad (2)$$

$$RI = \sum_{i=1}^{m} E_r^i \quad (3)$$

where C_f^i, T_r^i, and E_r^i represent the contamination factor, toxic response factor, and potential ecological risk factor, respectively, for the respective i^{th} heavy metal. Furthermore, C^i means the measured concentration of the heavy metal, while C_n^r C_n^r denotes the reference concentration associated with each heavy metal. The reference values for the Beibu Gulf region have previously been calculated based on uncontaminated preindustrial sediment samples (Xia et al., 2011) (Table S1). The toxic response factors for Hg, As, Cu, Cd, Cr, Pb, and Zn are 40, 10, 5, 30, 2, 5, and 1 (Hakanson, 1980). Additionally, the C_f^i was classified into four groups: C_f^i < 1: low contamination factor; C_f^i between ≥1 and < 3: moderate contamination factor; C_f^i between ≥3 and < 6: considerable contamination factor; C_f^i ≥ 6: very high contamination factor (Hakanson, 1980). The *RI* method (RI < 30: Low risk; 30 ≤ RI < 60: Moderate risk; 60 ≤ RI < 120: Considerable risk; RI ≥ 120: Very high risk) has been used previously to evaluate ecological risks caused by heavy metals in a variety of research domains, i.e. biological toxicology, environmental chemistry as well as ecology (Shi et al., 2010; Sun et al., 2010). Five categories of E_r^i and four classes of *RI* were defined, as shown in Table S1 (Huang et al., 2011).

2.3. DOM optical characterization and analysis

For analysis of the DOM pool, 3 g of homogenized sediment was suspended in 400 mL of Milli-Q water and thereafter filtered through a pre-combusted (450 °C, 6 h) GF/F (nominal pore size 0.7 μm, Whatman) filter. From this sediment extract, 20 mL were directly collected into two 40 mL glass vials and stored at −20 °C for subsequent dissolved organic carbon (DOC) and optical analysis. The remaining water, totalling 360 mL, was acidified to pH 2 in a 1 L glass bottle for solid phase extraction of DOM (SPE-DOM). For all DOM sample collection, storage and analysis glassware used were acid washed (2 % HCl for 24 h) and rinsed with Milli-Q water and precombusted (450 °C for 6 h) prior to use.

The coloured dissolved organic matter (CDOM) absorbance spectrum was recorded using a 2300 UV–visible spectrophotometer (Techcomp, China) with a 10-cm path-length quartz cuvette using ultrapure water as a reference. Absorbance spectra were baseline-corrected by subtracting the mean absorbance from 700 to 800 nm and converted to a absorption coefficients (in m^{-1}) by multiplying raw absorbance values by 2.303 and dividing by the cuvette path length. We used the absorption at 254 nm (a254) as a quantitative measure of the CDOM pool. The DOC-specific absorbance at 254 nm, known as $SUVA_{254}$ (ratio between absorbance at 254 nm and DOC) was used as an indicator of aromaticity (Weishaar et al., 2003). The CDOM fluorescence properties were characterized using excitation-emission matrices (EEMs) which were obtained on a Varian Cary Eclipse spectrofluorometer (USA). Fluorescence measurements were performed using a 1 cm quartz cuvette and EEMs were generated by scanning the emission spectra at 2 nm intervals within the wavelengths from 280 to 600 nm, at excitation wavelengths ranging from 240 to 450 nm at 5 nm intervals (Wang et al., 2017). The slit widths for both excitation and emission were set at 10 nm. Milli-Q water was

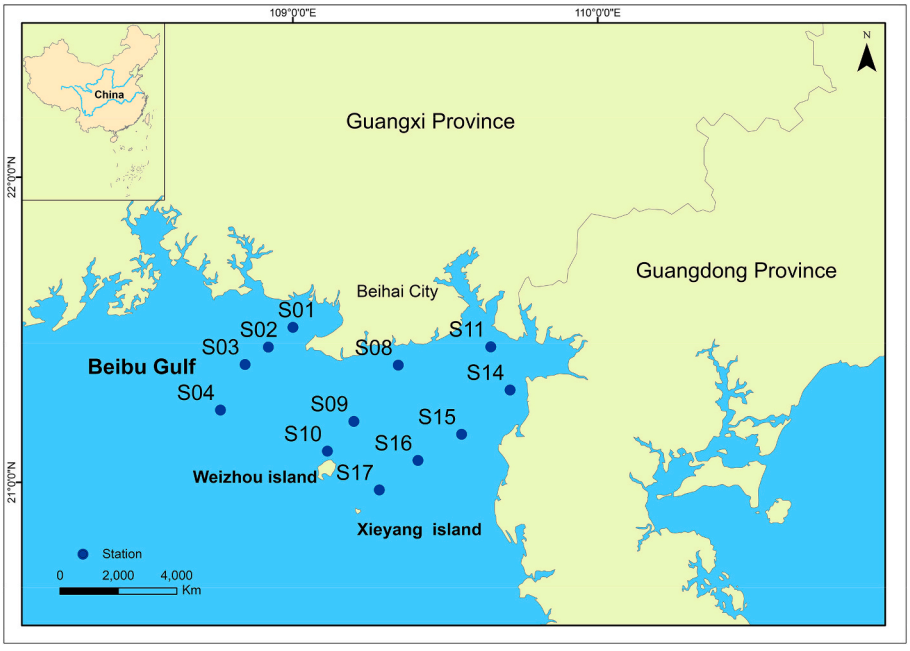

Fig. 1. Stations in the Beibu Gulf, South China Sea where surface sediment samples were collected during March 29–31, 2019.

used to generate blank EEMs. The EEMs and blank EEMs were scanned on the same day, and the sample EEMs were processed by subtracting the blank, and thereafter Raman normalized (Guo et al., 2014). The EEMs were decomposed into components using parallel factor analysis (PARAFAC), with Matlab 2012 and the DOMFluor toolbox (Stedmon and Bro, 2008). These components were compared with the OpenFluor database (http://www.openfluor.org). Moreover, a series of optical indices ($SUVA_{254}$, E2:E3, fluorescence index [FI], humification index [HIX], and autotrophic productivity [BIX]) were calculated to evaluate the quality of DOM, and their calculation and interpretation are provided in Table S4.

2.4. DOM sampling and FT-ICR MS measurement

The DOM filtrate was extracted using solid phase extraction (SPE) following previously published procedures (Dittmar et al., 2008). Briefly, 360 mL of acidified sample (pH 2) were extracted using cartridges (200 mg, Agilent Bond Elut PPL, USA). The SPE-DOM was eluted using 2 mL of high-pressure liquid chromatography-grade methanol (Sigma-Aldrich) and analyzed by Fourier transform ion cyclotron resonance mass spectrometer (FT-ICR MS) using a 9.4 T Bruker Apex Ultra with an Apollo II electrospray ion source operated in negative mode (He et al., 2020). The operating settings for the negative-ion ESI analysis include spray shield voltage (4.0 kV), capillary column introduced voltage (4.5 kV), and capillary column end voltage (320 V). Ions were accumulated in the collision cell for 0.2 s before being transferred into the ICR cell with a time-of-flight of 1.1 ms. In this setup the detected mass range is between 200 and 800 Da. The samples dissolved in methanol were injected into the electrospray source at an infusion flow rate of 250 μL/h and 128 single scans were added for each mass spectrum. Subsequently, a high-quality mass peak (m/z 371.0620 corresponding to $[C_{15}H_{16}O_{11}–H]^-$) at the centre of the mass range was selected as a reference peak. The resolution power of this peak was higher than 280.000. Two sets of mass peaks near the most abundant ones in the spectrum were selected to evaluate the relative abundance distribution. For calibration, the mass spectrometer was initially calibrated with sodium formate and recalibrated with a known mass series of the Suwannee River fulvic acids (SRFA), which provides a mass accuracy of 0.2 ppm or higher for the mass range of interest. The mass peaks with a signal-to-noise (s/n) ratio >4 were exported for formula assignment, while those with an s/n ratio >6 were selected for further analysis. The matched formulas consisted of the elemental combinations of $^{12}C_{1–60}$, $^{1}H_{1–120}$, $^{14}N_{0–3}$, $^{16}O_{0–30}$, and $^{32}S_{0–1}$. Relative intensities of double bond equivalents (DBE), H/C ratios, O/C ratios, as well as the modified aromatic index (AI_{mod}), were calculated for each sample as described previously (Wang et al., 2022). Additionally, relative intensity weighted m/z (m/z_{WM}), H/C (H/C_{WM}), O/C (O/C_{WM}), and AI_{mod} (AI_{modWM}) were calculated (Roth et al., 2019). The DOM molecular formulas (MFs) were assigned into different groups based on their properties (Antony et al., 2014): CRAM (carboxyl-rich alicyclic molecules, DBE/C = 0.30–0.68, DBE/H = 0.20–0.95, DBE/O = 0.77–1.75); HAC (Highly aromatics compounds, $0.5 \leq AI_{mod} < 0.67$); HUC (Highly unsaturated compounds, $H/C < 1.5$, $AI_{mod} \leq 0.5$); PCA (Polycyclic aromatics, $AI_{mod} \geq 0.67$); and Sat (Saturated compounds, $H/C > 2.0$). To distinguish the unique and common molecules in the contaminated and uncontaminated areas, we organized the categorized MFs into various groups depending on their occurrence in the two areas. The uniquely prevalent group contained the MFs that were detected in at least 50 % of the samples from the contaminated or the uncontaminated area but in less than half in the other area. For example, ‘uni con’ MFs group contained the MFs that occurred in more than three samples in the contaminated area but less than four samples in the uncontaminated area. Conversely, the common MFs group are those MFs that were found in more than half of the samples in both contaminated and uncontaminated areas.

2.5. DNA and RNA extraction and sequencing

The total bacterial community composition is represented by the DNA in the sample, while the metabolically active members are shown by analysis of RNA. Sediment genomic DNA and total RNA were extracted from the sediment samples (~2 g) according to the manufacturer’s instructions using DNeasy PowerSoil Pro Kit (Qiagen) and RNeasy PowerSoil Total RNA Kit (Qiagen), respectively. Subsequently, the RNA extracts were reverse transcribed into complementary DNA (cDNA) using the SuperScript IV kit (Invitrogen™) after being treated with TURBO™ DNase (Invitrogen™). The DNA and cDNA extracts were stored at −20 °C until further analysis.

The bacterial 16S rRNA and rDNA was amplified using the primers 515F (5′-GTGYCAGCMGCCGCGGTAA-3′) and 806R (5′-GGACTACNVGGGTWTCTAAT-3′). Archaeal 16S rRNA and rDNA amplification was conducted using the primers 519F (5′-CAGCCGCCGCGGTAA-3′) and 915R (5′-GTGCTCCCCCGCCAATTCCT-3′) (Zhang et al., 2021a). Triplicate PCR reactions for each sample were mixed to avoid bias. The amplicons were sequenced using the Illumina MiSeq PE300. Raw sequence analysis was performed using the QIIME2 pipeline (Version 2020.2) (Bolyen et al., 2019). After importing and demultiplexing, raw sequences were trimmed to a length of 250 bp, and low-quality sequences were removed (with default parameters). Then the sequences were denoised and clustered into amplicon sequence variants (ASVs) using the deblur function within QIIME2. The resulting feature table and reprehensive sequences were then assigned taxonomy using the trained SILVA database classifier (SILVA database release 132). Bacterial and archaeal 16S rRNA and rDNA sequences were deposited in NCBI SRA under BioProject number PRJNA1038687.

2.6. Statistical analysis

The difference in the composition of DOM MFs between the uncontaminated (S01, S02, S09, S10, and S17; definition in the result 3.1) and contaminated areas (S03, S04, S08, S11, S14, S15, and S16) was tested using the multi-response permutation procedure (MRPP) with 999 permutations. The correlation between microbial community diversity (Shannon index) and the concentration of heavy metals, as well as DOM properties, was calculated using Spearman correlations. Redundancy analysis (RDA) was performed to explore the relationship between the structure of the microbial community and DOM properties, as well as the concentrations of heavy metals using the vegan package. The linear discriminant analysis Effect Size (LEfSe) was used to detect the major bacteria/archaea groups contributing to the dissimilarities observed in microbial communities between uncontaminated and contaminated areas (Segata et al., 2011). Principal coordinates analysis (PCoA) and permutational analysis of variance (PERMANOVA) were used to determine the similarity of samples to each other based on Bray-Curtis dissimilarities using the vegan package. All statistical analysis was performed in R (www.R-project.org).

The construction of the co-occurrence network between microbial communities and DOM MFs was performed based on Spearman correlations followed by post-hoc test using the false-discovery-ratio (FDR) test using the R packages igraph, WGCNA, and fdrtool. To enhance confidence, only the ASV and DOM MFs that were present in at least 7 samples were retained in the network construction. Subsequently, correlation with an $|r| > 0.7$ and FDR q-value < 0.05 was retained for further analysis.

3. Results

3.1. Sediment heavy metal concentrations

Seven heavy metals were detected in the sampled surface sediments, including Hg, Cu, Cr, Zn, As, Cd, and Pb (Fig. 2). From the coast to the further offshore stations, heavy metal concentrations increased in our

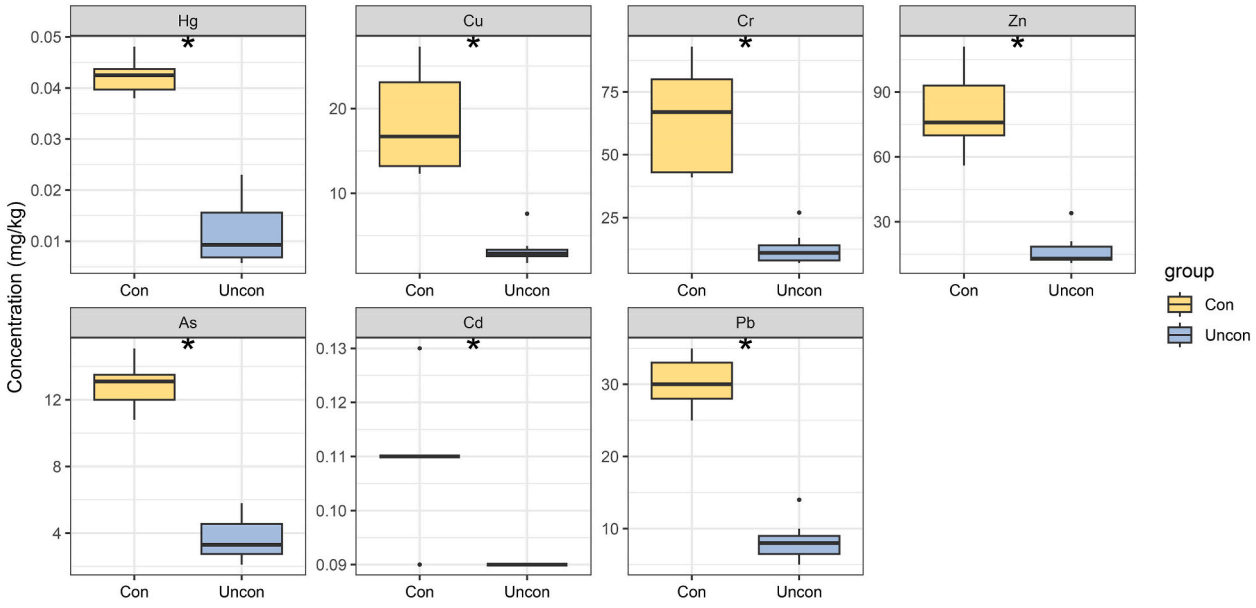

Fig. 2. Box-and-whiskers plots of concentrations of heavy metals (mercury (Hg), copper (Cu), chromium (Cr), zinc (Zn), arsenic (As), cadmium (Cd), and lead (Pb))in the surface sediment of the Beibu Gulf. Fifty percent of the data are included within the limit of the boxes, and the two ends of the box are represented by the upper quartile (25th percentiles) and the lower quartile (75th percentiles), while the solid line within the box represents the median value. The contaminated area (Con) includes stations S01, S02, S09, S10, and S17, while uncontaminated (Uncon) stations includes stations S03, S04, S08, S11, S14, S15 and S16. Asterisk indicates the *p*-value of the *t*-test <0.05.

transect section 2 and 3 but decreased in section 1. Higher metal concentrations were generally detected at stations closer to harbours or islands. For instance, S01 and S02 were located near the harbour of Beihai City, S09 and S10 were in proximity to Weizhou Island, and S17 was close to Xieyang Island. Generally, the *RI* factor in four stations, including S01, S02, S09 and S10 exceeded 60, indicating a considerable potential ecological risk (Table S3). The E_r^i factor indicated that Hg, As and Cd were the major contributors to the potential ecological risk (Table S3). Additionally, the *RI* factor of S17 (32.5) indicated a moderate risk. Specifically, the contamination factors (C_f^i) of Cr, Zn, Cd, and Pb exceed 1 at stations located near harbours or islands (Table S1), indicating the pollution of these heavy metals. Examples of this are the C_f^i factor of Cr which exceeded 1 at stations S09, S10, and S17, while the contamination factor of Zn exceeded 1 at stations S01, S09, S10, and S17 (Table S1). Following these results we in this manuscript define the contaminated (*RI* > 30; S01, S02, S09, S10, and S17) and uncontaminated (*RI* < 30; S03, S04, S08, S11, S14, S15, and S16) areas (Table S3).

3.2. Dissolved organic carbon and optical properties

Similar DOC concentrations were measured in the uncontaminated (0.041 ± 0.012 mg/g) and contaminated area (0.044 ± 0.033 mg/g) (Fig. S1, Wilcoxon test, *p*-value >0.05), and concentrations were not related with the heavy metal concentrations (Fig. S2). Two fluorescent DOM (FDOM) components were identified using PARAFAC analysis (Fig. S1). Component C1 (Ex/Em wavelengths: 275/350 nm) was characterized as protein-like (Groeneveld et al., 2020; Kothawala et al., 2014), while component C2 (Ex/Em wavelengths: 275/450 nm) was defined as humic-like FDOM (Jørgensen et al., 2011; Lin and Guo, 2020). There was no significant difference in the relative intensity of these two components between contaminated and uncontaminated areas (Fig. S1). Furthermore, most DOM optical proxies in the contaminated area were similar to those in the uncontaminated area (Fig. S1). However, FI was significantly higher in the uncontaminated area compared with the contaminated area (Wilcoxon test, *p*-value = 0.03), and FI was significantly correlated with the heavy metal concentrations (Fig. S2).

3.3. Dissolved organic matter composition

A total number of 4865 MFs were detected by FT-ICR MS across all samples (Table S5). A higher number of MFs was found in the contaminated area (3317 ± 327) compared to the uncontaminated area (2356 ± 684) (Wilcoxon test, *p*-value = 0.02; Fig. 3). Additionally, the contaminated area displayed higher values of O/C and O/C_{WM} compared to the uncontaminated area (Fig. 3). The MFs were categorized into different groups based on their properties. The contaminated area had more CRAM and HUC but fewer HAC MFs (Wilcoxon test, *p*-value <0.05; Fig. S3) compared to the uncontaminated area. Overall the DOM molecular composition in the contaminated area was different from that in the uncontaminated area as revealed by our PCoA analysis (Fig. 4b). The MRPP analysis also showed a significant difference in the DOM composition between the contaminated and uncontaminated areas (*p*-value = 0.02). Compared to the contaminated area, the DOM composition in the uncontaminated area was more variable as revealed by PCoA (Fig. 4b). To demonstrate this difference, we grouped the categorized MFs into several groups based on the presence in the two areas. The uniquely prevalent group contained the MFs that were detected in at least half of the samples in the contaminated or the uncontaminated area but in less than half in the other area (uni con and uni uncon). Contrary the common MFs group are those that were found in more than half of the samples in both contaminated and uncontaminated areas. In the contaminated area (uni con MFs) the DOM pool had significantly higher *m/z*, O/C, AI_{mod}, and DBE compared to the uncontaminated area (uni uncon MFs) (Fig. 4). Furthermore, in the contaminated area (uni con) the DOM pool had a higher proportion of nitrogen- and sulfur-containing molecules than the uncontaminated area (uni uncon) (Fig. 4 and Table S6). These results suggest that sediment heavy metal contamination could lead to a more homogenized DOM chemical composition, which significantly differs from the composition observed in uncontaminated sediments.

3.4. Structure of total and active microbial communities

A total number of 317,804 and 155,565 high-quality sequences of

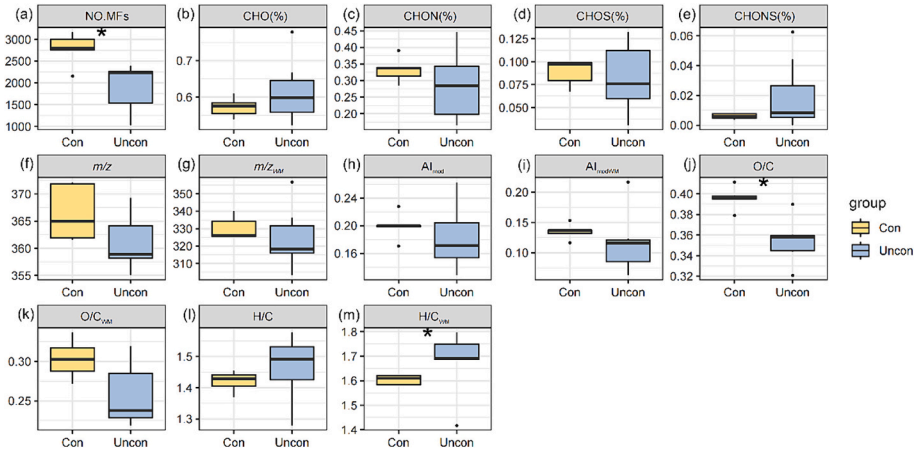

Fig. 3. Box-and-whiskers plots of sediment dissolved organic matter chemical properties in the Beibu Gulf. The a) number of the molecular formula (NO.MFs), b) the average percentage of CHO formulas (CHO%), c) the average percentage of CHON formulas (CHON%), d) the average percentage of CHOS formulas (CHOS%), e) the average percentage of CHONS formulas (CHONS%), f) mass-to-charge ratio (m/z), g) mass-to-charge ratio calculated with weighting factors (m/z_{WM}), h) the modified aromatic index (AI_{mod}), i) the modified aromatic index calculated with weighting factors (AI_{modWM}), j) oxygen to carbon ratio (O/C), k) oxygen to carbon calculated with weighting factors (O/C_{WM}), l) ratios of hydrogen to carbon (H/C), m) ratios of hydrogen to carbon calculated with weighting factors (H/C_{WM}). Fifty percent of the data are included within the limit of the boxes, and the two ends of the box are represented by the upper quartile (25th percentiles) and the lower quartile (75th percentiles), while the solid line within the box represents the median value. Asterisk indicates the significance value <0.05 by Wilcoxon test. Con means the contaminated area including stations S01, S02, S09, S10, and S17, while Uncon means the uncontaminated area including stations S03, S04, S08, S11, S14, S15 and S16.

bacteria and archaea were obtained, respectively. Both the total and active bacterial communities of Beibu Gulf sediments were dominated by Gamma- (45 % and 57 %, respectively) and Delta-proteobacteria (18 % and 16 %) (Fig. 5a), while the archaeal communities were dominated by Nitrosophaeria (45 % and 51 %) and Bathyarchaeia (20 % and 27 %) (Fig. 5b). Within the uncontaminated area, Gammaproteobacteria (30 % and 46 %), Deltaproteobacteria (25 % and 19 %, respectively), and Clostridia (6 % and 9 %) dominated. While in the contaminated area, Gammaproteobacteria (56 % and 64 %), Deltaproteobacteria (13 % and 13 %), and Alphaproteobacteria (5 % and 4 %) comprised a major proportion of the total and active bacterial communities. In the uncontaminated area, the major proportion of both total and active archaeal communities were Bathyarchaeia (30 % and 47 %), Nitrosophaeria (26 % and 22 %) and Woesearchaeia (21 % and 7 %). While in the contaminated area, the dominant total and active archaeal communities consisted of Nitrososphaeria (60 % and 72 %), Woesearchaeia (17 % and 4 %) and Bathyarchaeia (13 % and 17 %). We found that there was no significant difference in the Shannon index of the bacterial community between the contaminated area and the uncontaminated area (Fig. 5c). In contrast, the Shannon index of both total and active archaeal communities increased in the contaminated area than in the uncontaminated area (Fig. 5c). We used LEfSe analysis to identify indicator taxa associated with the microbial community changes in each area (Fig. S4). The analysis revealed that the relative abundances of two archaeal groups increased in response to increasing heavy metal concentrations, i.e., the phyla Euryarchaeota (mainly the class Methanobacteria and Methanomicrobia) and Diapherotrites (mainly the class Iainarchaeia). Additionally, five lineages of bacteria including the phyla Proteobacteria, Gemmatimonadetes, Calditrichaeota, Actinobacteria, and Schekmanbacteria, were enriched in response to increasing heavy metal concentrations. The PCoA results revealed that there were similar structures of the bacterial and archaeal communities between uncontaminated and contaminated areas (PERMANOVA, p-value >0.05; Fig. 5d–g).

3.5. Links between dissolved organic matter and microbial communities

To further investigate potential linkages between the microbial community and DOM molecules, networks based on Spearman's rank correlation coefficient were constructed (Fig. 6). Interestingly, we found that DOM molecules had a tighter coupling with bacterial communities than archaeal communities. No significant correlation was detected between DOM molecules and the total archaeal ASVs. The active-bacteria-DOM network showed a higher number of nodes and connections compared to the total-bacteria-DOM network. Furthermore, greater numbers of nodes and connections were found in the active-bacteria-DOM network than in the active-archaea-DOM network (Fig. 6a and b). These results suggest that DOM molecules might be more closely associated with active microbes than the whole community. Therefore, we in the following analysis focused on networks based on active bacteria and archaea.

A total number of 301 and 105 ASVs belonging to active bacteria and archaea were found in the networks, respectively. Within these networks, Gama-, Delta- and Alpha-proteobacteria were the dominant bacterial groups (73 %, 17 % and 29 %), while in the active archaeal community Nitrososphaeria (59 %) and Bathyarchaeia (35 %) dominated. The ASVs affiliated with Gammaproteobacteria and Alphaproteobacteria in the bacteria-DOM network showed a higher average relative abundance in the contaminated area (64 % and 4 %) than uncontaminated area (45 % and 3 %). Whereas, the ASVs affiliated with Deltaproteobacteria revealed a lower average relative abundance in the contaminated area (13 %) compared to uncontaminated area (19 %). Within archaea-DOM network, the ASVs affiliated with Nitrososphaeria showed a higher average relative abundance in the contaminated area (72 %) than uncontaminated area (22 %). However, the ASVs affiliated with Bathyarchaeia revealed a lower average relative abundance in the contaminated area (14 %) compared to the uncontaminated area (47 %). A total number of 756 and 455 MFs were correlated with active bacteria and archaea, respectively. Furthermore the MFs correlated with active bacteria revealed a similar proportion of CHO molecules to that correlated with active archaea (Table S6). However, a higher proportion of CHON molecules and a lower proportion of CHOS molecules were observed in the bacteria-DOM compared to the archaea-DOM network. Moreover, we found higher values of AI_{mod}, m/z, O/C, and DBE in the bacteria-DOM than in the archaea-DOM network. More CRAM but less highly aromatics compounds (HAC) were found in the bacteria-DOM compared to the archaea-DOM network (Fig. 6c and d). Additionally, the contaminated area contained more CRAM and fewer HAC than the uncontaminated area (Fig. S3). These results suggest that active bacteria

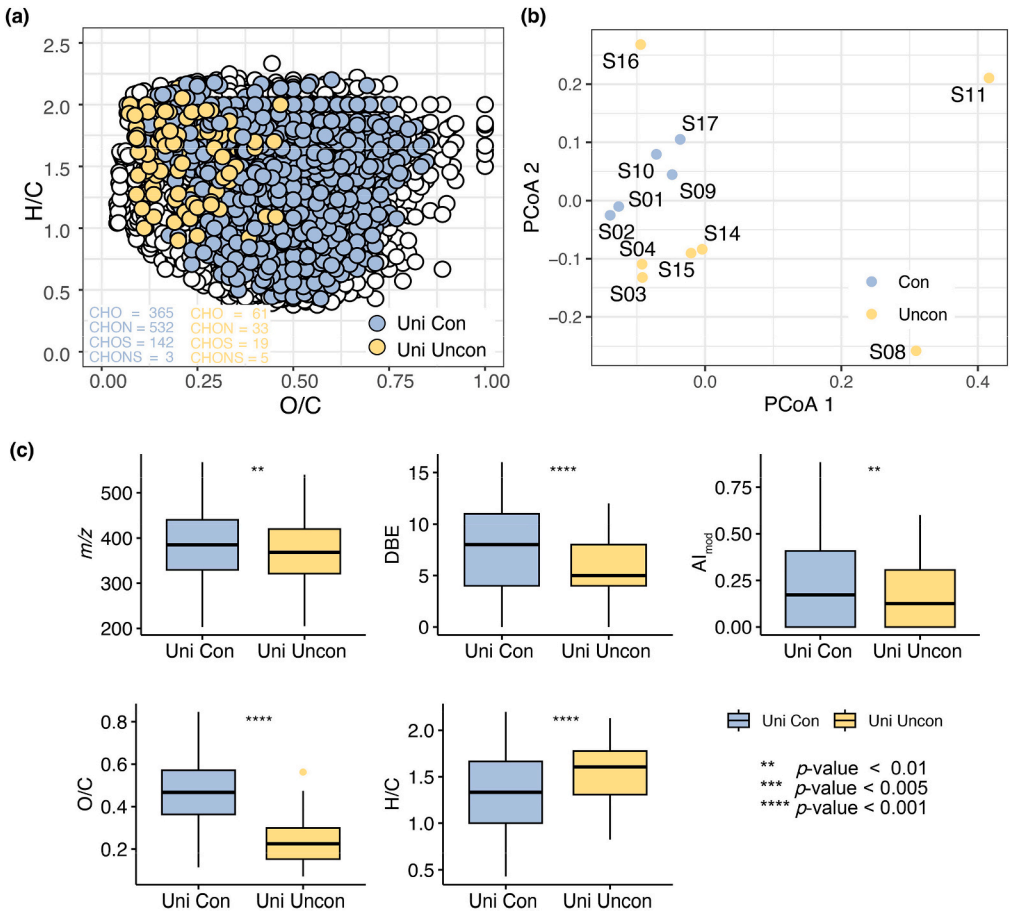

Fig. 4. Structure and properties of the DOM molecular formulas (MFs) in the Beibu Gulf sediments. a) the Van Krevelen plot highlights the MFs in the Beibu Gulf sediments, which are unique in the contaminated (Uni Con) and uncontaminated areas (Uni Uncon). b) The principal coordinate decomposition analysis (PCoA) shows the difference in the DOM MFs composition based on the Bray-Curtis dissimilarity of the MFs. c) Box-and-whiskers plot of DOM MFs properties unique in the contaminated area (Uni Con) and uncontaminated area (Uni Uncon) are shown. Here the contaminated area includes stations S01, S02, S09, S10, and S17, while the uncontaminated area includes stations S03, S04, S08, S11, S14, S15 and S16. In c) 50 % of the data are included within the limit of the boxes, and the the two ends of the box are represented by the upper quartile (25th percentiles) and the lower quartile (75th percentiles), while the solid line within the box represents the median value. Asterisk shows the significance of the difference in each property determined using *t*-test.

in these sediments were more involved in the transformation and/or production of recalcitrant DOM compared to active archaea.

4. Discussion

In coastal waters, sediments are key components players in the cycling of inorganic and organic matter as well as the storage of contaminates such as heavy metals. At the center of all these processes are the interactions between microbes and DOM. Assessing the impact of heavy metal pollution on these interactions is therefore essential for understanding and maintaining coastal ecosystem health and functioning.

4.1. Sediment heavy metals

The influx of heavy metals is having adverse effects on coastal waters globally, influencing all parts of the foodweb (Le et al., 2022). Our measurements of heavy metals suggest that these pose a moderate ecological risk in the Beibu Gulf region. Specifically, we observed higher concentrations of certain heavy metals, including Cr, Zn, Pb, and Cd, in the sediments closer to land-based human activities in the northern Gulf (Table S1), as was also suggested by several previous studies in the same region (Dou et al., 2013; Lin et al., 2021; Liu et al., 2020).

4.2. Impacts of heavy metals on microbial communities

Toxicity of heavy metals has previously been shown to change the microbial community composition in surface sediments (Dell'Anno et al., 2020; Wang et al., 2021b). Similarly in our study, we found that elevated heavy metal concentrations impacted the archaeal community diversity, while contrary no impact was found on the bacterial community (Figs. 5 and S2). These contrasting impacts are similar to previous observations in sediment from a Norwegian fjord (Gillan et al., 2005) and it supports the hypothesis that archaeal communities have greater sensitivity to heavy metals than bacterial communities (Long et al., 2021).

While overall the archaeal community showed higher heavy metals sensitivity, certain groups within the community had the ability to tolerate such conditions. Specifically, we found a rise in the relative abundances of two archaeal groups, namely the phyla Euryarchaeota and Diapherotrites, with increasing heavy metal concentrations (Fig. S4). This enrichment suggests that they have a higher tolerance, which is in line with previous studies showing that Euryarchaeota prevails in metal-rich environments (Li et al., 2017; Yang et al., 2014), likely due to their utilization of P-type ATPases and ABC transporters for metal transport and homeostasis (Contursi, 2013; Coombs and Barkay, 2005). However, it is here worth noticing that the metal tolerance of Euryarchaeota may differ between species (Cornall et al., 2016). Thaumarchaeota, another prevalent archaea in our study, has been

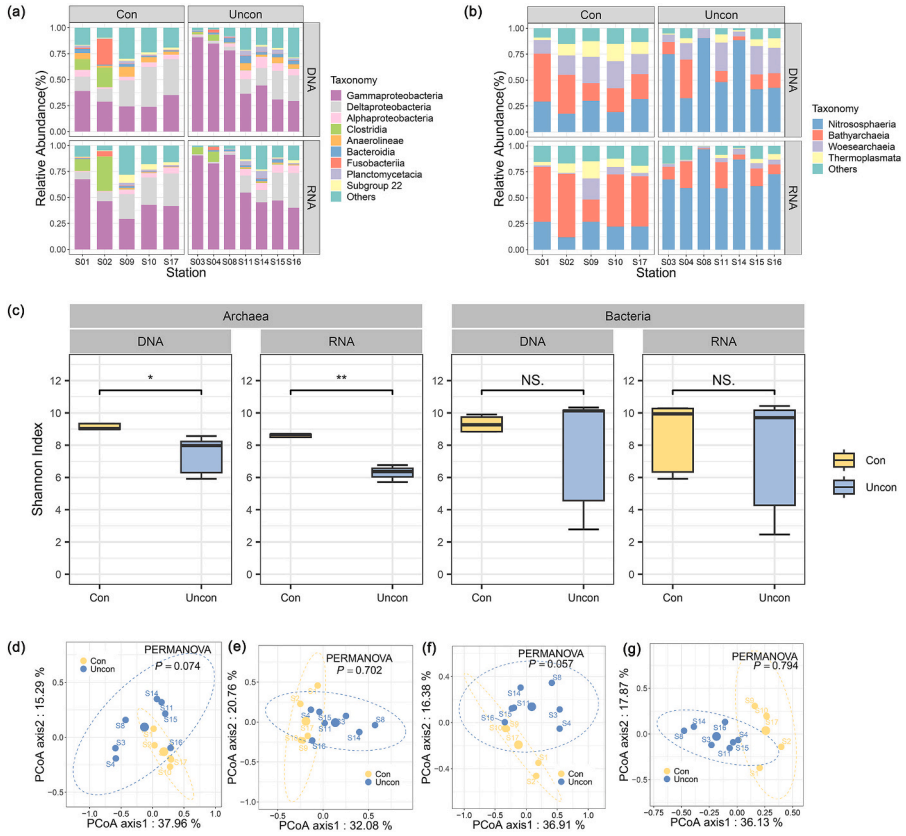

Fig. 5. Composition (a and b) and diversity (c–g) of the total and active bacterial and archaeal communities in the surface sediments in the Beibu Gulf. The a) total and active bacterial communities, as well as the b) archaeal communities are shown together with the c) Box-and-whiskers plot of the Shannon index of these communities in surface sediments of the Beibu Gulf. The Principal coordinate analysis of Bray-Curtis distances of the d) total and f) active bacterial communities and e) total and g) active archaeal communities. Here the contaminated area includes stations S01, S02, S09, S10, and S17, while the uncontaminated area includes stations S03, S04, S08, S11, S14, S15, S16. In c) 50 % of the data are included within the limit of the boxes, error bars are the 95% confidence interval, the bottom and top of the box are the 25th and 75th percentiles, the line inside the box is the 50th percentile (median). Asterisk indicates a *p*-value <0.05, while double asterisk indicates a *p*-value <0.01

discovered in metal-rich sediments, suggesting that they are capable of tolerating high heavy metal concentrations (Subrahmanyam et al., 2014; Volant et al., 2012). However, the concrete impact of heavy metals on Thaumarchaeota is still unresolved with some studies reporting high sensitivity (Liu et al., 2018; Wang et al., 2018), while others suggest they are resistant (Subrahmanyam et al., 2014). In our study, we observed a higher relative abundance of Thaumarchaeota in the contaminated area, while the uncontaminated area had a higher contribution of Nitrososphaeria (within the phylum Thaumarchaeota). Therefore, the impact of heavy metals on the phylum level (Thaumarchaeota) might not represent outcomes for all lineages and further research is therefore needed to gain a deeper understanding of the concrete ecological effects.

Although no significant correlation was observed between the diversity of the bacterial communities and the heavy metal concentrations, certain bacterial species exhibited clear responses. Specifically, the bacterial lineages, particularly Proteobacteria and Gemmatimonadetes, play crucial roles in heavy metal degradation and are also widespread in wastewater treatment plants (Acosta-González et al., 2013; Kostka et al., 2011; Zeng et al., 2022). Actinobacteria and Calditrichaeota, known for their high metal resistance (Alvarez et al., 2017; Margesin et al., 2011; Marshall et al., 2017), were notably abundant in the contaminated areas. Moreover, we observed high relative abundances of Anaerolineae, Bacteroidia, and Planctomycetacia in our study areas. All these bacterial classes have previously been reported as dominant community members in contaminated sediments (Ren et al., 2016; Zhang et al., 2021b), attributed to their role as heavy metal reducers, polyaromatic compounds degraders and their ability to survive toxic effects of metals (Nogales et al., 2007; Petrie et al., 2003; Zanaroli et al., 2012; Zhao et al., 2018a). Collectively, our results indicate that the diversity of archaeal communities, as well as specific bacterial and archaeal species, shifts due to the presence of heavy metals, which may consequently change the microbial mediated biogeochemical cycles.

4.3. Interactions between heavy metals, microbes and dissolved organic matter

In marine sediments the DOM chemical composition is tightly coupled with the microbial community structure (Tang et al., 2022). In our study, we found noticeable differences in the DOM chemical composition between contaminated and uncontaminated areas (Fig. 3 and S3). Furthermore, our network analysis demonstrates distinct associations between bacterial and archaeal communities with specific DOM chemical groups (Fig. 6 and Table S6). Our results suggest a stronger relationship between active bacteria and recalcitrant DOM than for archaea. Interestingly, our results contradict a previous study investigating Pearl River estuarine sediments, which reported a stronger connection between archaea and recalcitrant DOM (Wang et al., 2021a). These contrasting results could be due to differences in sediment biological and chemical composition, main organic matter sources and/or the environmental conditions. Furthermore, the Pearl River Estuary, has over the past four decades, been impacted by heavy loading of e.g. Organic pollutants and heavy metals (Chen et al., 2018; Gan et al., 2013;

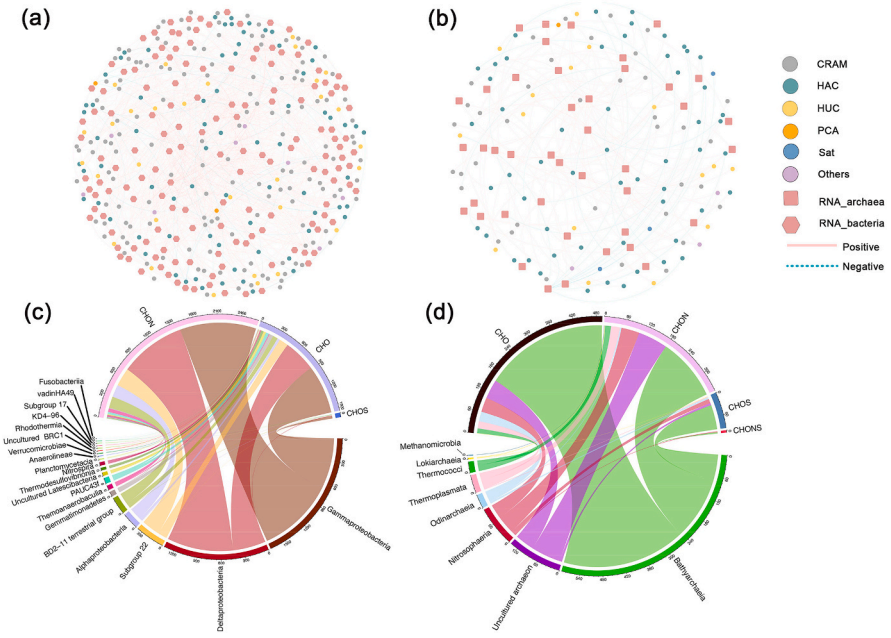

Fig. 6. Co-occurrence network that represents the links between DOM properties and the active bacterial (a and c) or archaeal communities (b and d). Significant Spearman correlation (q-value <0.01, and $r > 0.7$) are represented. The color of the circle nodes represents the molecular formula group: grey, carboxyl-rich alicyclic molecules (CRAM); green, highly aromatics compounds (HAC); light orange, highly unsaturated compounds (HUC); purple, other components; dark orange, polycyclic aromatics (PCA); blue, saturated compounds (Sat). The pink hexagonal nodes represent bacteria, while the pink square nodes represent archaea.

Lao et al., 2019). In contrast, our study area, the Beibu Gulf, is a semi-closed area with proportionally lower pollution levels than those in the Pearl River Estuary (Lin et al., 2021; Zhao et al., 2018b). Previous studies have also found that Hg and Cd are the main heavy metals in the sediments of the Pearl River Estuary (Xiao et al., 2022a; Zhao et al., 2018b), while in our study area Cr, Zn, Cd, and Pb dominated. In addition, Our results revealed that chromium (Cr), zinc (Zn), cadmium (Cd), and lead (Pb) were the heavy metals contributing to pollution in our studied area, with average concentrations (mg/kg) of 34.4 (Cr), 43.8 (Zn), 0.1 (Cd) and 17.4 (Pb). Notably, the average concentrations of these four heavy metals in the Pearl River Estuary sediments are significantly higher than in the Beibu Gulf. For instance, Liang et al.'s study reported that the average concentrations of Cr, Zn, and Pb were 118.5, 198.5, and 73.0, respectively (Liang et al., 2023), and in the study conducted by Xiao et al., the average concentrations were 73.63 (Cr), 119.24 (Zn), 0.24 (Cd) and 24.05 (Pb) (Xiao et al., 2022b). This therefore suggests that differences in heavy metal presence and concentration in sediments between regions could lead to differences in the microbial composition and DOM properties.

The dominant microbial communities in the bacteria-DOM network consisted of three active bacterial groups: Gammaproteobacteria (73 %), Deltaproteobacteria (17 %), and Alphaproteobacteria (4 %), which also in previous studies have been shown to play key roles in organic matter degradation (Basak et al., 2015; Chen et al., 2022). Gammaproteobacteria, which contains diverse groups has been shown capable of adapting to high heavy metal environments, while still actively transforming nitrogen- and sulfur-containing organic matter (Li et al., 2018). Among these groups is the B2M28 (within class Gammaproteobacteria), which in our study was found to be a good "contamination indicator" identified by LEfSe analysis (Fig. S4 and Table S7). This group furthermore has a close relationship with nitrogen-containing molecules and HAC compounds (Table S7) and it has previously been shown to be a keystone player within networks of bacteria and fungi in Beibu Gulf sediments (Zhao et al., 2022). Therefore, our findings suggest that this group could be a good indicator of heavy metal pollution. Since there is limited study on its relationship with nitrogen-containing molecules and HAC compounds, future research on heavy metal pollution should pay increased attention to this group. Additionally, the Gammaproteobacteria class has been shown to play a vital role in the oxidation of sulfides and the degradation of pollutants (Sazykin et al., 2023). This was confirmed in our study where the Oceanospirillales group belonging to the Gammaproteobacteria class was found to be associated with (42 %) sulfur-containing molecules and they had a higher relative abundance in areas with higher heavy metal concentrations. Our findings also revealed that sulfur-oxidizing bacteria (Woeseia and Thiohalophilus, affiliated with Gammaproteobacteria) and sulfur-reducing bacteria (Desulfuromonadaceae, Desulfobacteraceae, Desulfobulbaceae, and Desulfatiglans, affiliated with Deltaproteobacteria) were more abundant in the contaminated area compared to the uncontaminated area (Table S8), which suggests that bacterial sulfur cycling could be affected by heavy metals. In addition, Deltaproteobacteria, predominately members of the Desulfobacterales, were highly related to CHON-containing molecules in our study, consistent with previous studies showing the most microdiversity of associated nifH sequences (Kapili et al., 2020). Rhodobacterales (within class Alphaproteobacteria), which in our study had a higher presence in the uncontaminated area (Fig. S4 and Table S7), exhibited a strong association with nitrogen-containing molecules and a comparatively weaker association with CRAM molecules (Table S7). This finding is well in line with studies demonstrating that Rhodobacterales might be less competitive when substrates are more recalcitrant (Xu et al., 2022). Generally, Alphaproteobacteria are known to possess several copies of nitroreductase-encoding genes which are involved in the reduction of nitrogen-containing aromatic compounds, and their genomes also exhibit numerous important sulfur metabolic functions (Karimi et al., 2019). Overall, our findings indicate that increase in Gammaproteobacteria and Alphaproteobacteria due to heavy metal contamination could affect the transformation of nitrogen- and sulfur-containing as well as aromatic DOM component. These diverse metabolic capabilities might enhance their ability to produce more recalcitrant DOM compounds (Chen et al., 2023; Wang et al., 2021b).

As for the archaea-DOM network, Nitrososphaeria (59 %) and Bathyarchaeia (35 %) were the dominant groups. We found that DOM molecules belonging to CRAM-like structures were correlated to Bathyarchaeia (41 %), which has been proposed to mediate the degradation

of recalcitrant organic matter (Saw et al., 2020; Yu et al., 2018). Additionally, a high proportion of HAC (42 %) was found to be associated with Bathyarchaeia in the archaea-DOM network, consistent with their known ability to utilize aromatic compounds (Meng et al., 2014; Zhou et al., 2018). Comparative genomics studies have also revealed that Bathyarchaeia genomes encode a large variety of genes related to carbohydrate degradation, especially playing an important role in lignin degradation in anoxic sediments (Yu et al., 2023). The higher relative abundance of Bathyarchaeia in the contaminated area compared to the uncontaminated area suggests that they are also capable of tolerating heavy metals (Table S9). Nitrososphaeria showed a stronger correlation with CRAM-like compounds (26 %), but their relative abundance decreased in the contaminated area, which fits well with previous studies showing that members of Nitrososphaeria are more abundant in uncontaminated areas (Moreira et al., 2023; Tangherlini et al., 2020). Suppression of this archaeal group by heavy metals may impact the transformation of CRAM-like, as well as nitrogen- and sulfur-containing DOM compounds (Table S9).

Bacteria and archaea residing in sediments are directly involved in the transformation and mineralization of organic matter (Mahmoudi et al., 2017), whereby they impact both the quality and quantity of these compounds (Koho et al., 2013). These microbial processes have profound consequences for both local and global biogeochemical cycles in sediments (Burdige, 2007). For example, processes mediated by microbes and exoenzymes can catalyze the transformation of high molecular weight DOM into low molecular weight compounds (Arnosti, 2004). The outcomes of our research imply that the presence of heavy metals leads to a modification in the structure of the local microbial community, particularly the archaeal community. This alteration impacts the microbial communities' capacity to mediate elemental cycling, resulting in changes in the composition of the DOM pool in coastal sediments. Our results indicate that the heavy metal pollution would accumulate more recalcitrant DOM and elevate the stability of DOM in the coastal sediments, which is more beneficial to long-term carbon storage. Moreover, the reduced bioavailability of DOM in the surface sediment could be transported into coastal bottom seawater by resuspension, potentially impacting the benthic food web (Hyun et al., 2022) and subsequently influencing the coastal ecosystem. Our research underscores the critical role of both microbial communities and DOM in the carbon cycling process as well as the impact of contaminates. Our results also suggest that heavy metal presence significantly affects the application of nitrifier-enriched activated sludge (NAS) for wastewater treatment (Sepehri et al., 2020; Sepehri and Sarrafzadeh, 2018). Overall, the observed changes in microbial and DOM composition, attributable to heavy metal contamination, could have implications for carbon storage and release mechanisms, which in turn could impact global carbon cycling dynamics, however, these links need urgently to be investigated in more detail.

5. Conclusions

In this study, we investigated how heavy metals influence microbe-DOM interactions in coastal surface sediments. We found that Zn, Cr, Cd, and Pb were the major heavy metals in the Beibu Gulf surface sediments. Interestingly our detailed chemical analysis revealed a higher proportion of CRAM and higher O/C_{WM} of DOM molecules in the contaminated area, suggesting accumulation of recalcitrant DOM in areas with elevated heavy metal concentrations. Our results also clearly demonstrate that heavy metals change the structure and diversity of archaeal communities while the bacterial communities were largely unaffected. Combined the detailed chemical and microbial analysis revealed that increasing heavy metal concentrations disrupted the interactions between the DOM pool and the microbial community leading to a convergent composition of DOM that is distinct and contains more recalcitrant compounds.

CRediT authorship contribution statement

Yu Wang: Writing – review & editing, Writing – original draft, Visualization, Methodology, Funding acquisition. **Yuxing Hu:** Writing – original draft, Visualization, Methodology, Writing – review & editing. **Yanting Liu:** Methodology, Data curation. **Qi Chen:** Software, Methodology. **Jinxin Xu:** Methodology, Data curation. **Fei Zhang:** Investigation, Data curation. **Jinhua Mao:** Writing – review & editing. **Quan Shi:** Methodology, Conceptualization. **Chen He:** Methodology, Conceptualization. **Ruanhong Cai:** Methodology, Conceptualization. **Christian Lønborg:** Writing – review & editing, Funding acquisition. **Lihua Liu:** Data curation. **Aixing Guo:** Visualization. **Nianzhi Jiao:** Resources. **Qiang Zheng:** Writing – review & editing, Methodology, Funding acquisition, Conceptualization.

Declaration of competing interest

The authors declare that they have no known competing financial interests or personal relationships that could have appeared to influence the work reported in this paper.

Data availability

Data will be made available on request.

Acknowledgment

This work was supported by the National Natural Science Foundation of China (92251306, 42188102, 42106138, and 42222604), the Chinese Academy of Sciences (project XK2022DXA001), the Project of Environmental Protection Science and Technology of Fujian Province of China (2023R002), and the China Postdoctoral Science Foundation (2020M671943). CL was during the writing of this manuscript supported by the Independent Research Fund Denmark Grant (1127-00033B).

Appendix A. Supplementary data

Supplementary data to this article can be found online at https://doi.org/10.1016/j.scitotenv.2024.172003.

References

Acosta-González, A., Rosselló-Móra, R., Marqués, S., 2013. Characterization of the anaerobic microbial community in oil-polluted subtidal sediments: aromatic biodegradation potential after the prestige oil spill. Environ. Microbiol. 15, 77–92. https://doi.org/10.1111/j.1462-2920.2012.02782.x.

Alvarez, A., Saez, J.M., Davila Costa, J.S., Colin, V.L., Fuentes, M.S., Cuozzo, S.A., Benimeli, C.S., Polti, M.A., Amoroso, M.J., 2017. Actinobacteria: current research and perspectives for bioremediation of pesticides and heavy metals. Chemosphere 166, 41–62. https://doi.org/10.1016/j.chemosphere.2016.09.070.

Antony, R., Grannas, A.M., Willoughby, A.S., Sleighter, R.L., Thamban, M., Hatcher, P.G., 2014. Origin and sources of dissolved organic matter in snow on the East Antarctic ice sheet. Environ. Sci. Technol. 48, 6151–6159. https://doi.org/10.1021/es405246a.

Arnosti, C., 2004. Speed bumps and barricades in the carbon cycle: substrate structural effects on carbon cycling. Mar. Chem. 92, 263–273. https://doi.org/10.1016/j.marchem.2004.06.030.

Basak, P., Majumder, N.S., Nag, S., Bhattacharyya, A., Roy, D., Chakraborty, A., SenGupta, S., Roy, A., Mukherjee, A., Pattanayak, R., Ghosh, A., Chattopadhyay, D., Bhattacharyya, M., 2015. Spatiotemporal analysis of bacterial diversity in sediments of sundarbans using parallel 16S rRNA gene tag sequencing. Microb. Ecol. 69, 500–511. https://doi.org/10.1007/s00248-014-0498-y.

Bolyen, E., Rideout, J.R., Dillon, M.R., Bokulich, N.A., Abnet, C.C., Al-Ghalith, G.A., Alexander, H., Alm, E.J., Arumugam, M., Asnicar, F., Bai, Y., Bisanz, J.E., Bittinger, K., Brejnrod, A., Brislawn, C.J., Brown, C.T., Callahan, B.J., Caraballo-Rodríguez, A.M., Chase, J., Cope, E.K., Da Silva, R., Diener, C., Dorrestein, P.C., Douglas, G.M., Durall, D.M., Duvallet, C., Edwardson, C.F., Ernst, M., Estaki, M., Fouquier, J., Gauglitz, J.M., Gibbons, S.M., Gibson, D.L., Gonzalez, A., Gorlick, K., Guo, J., Hillmann, B., Holmes, S., Holste, H., Huttenhower, C., Huttley, G.A., Janssen, S., Jarmusch, A.K., Jiang, L., Kaehler, B.D., Kang, K.B., Keefe, C.R., Keim, P., Kelley, S.T., Knights, D., Koester, I., Kosciolek, T., Kreps, J., Langille, M.G.I., Lee, J., Ley, R., Liu, Y.-X., Loftfield, E., Lozupone, C., Maher, M., Marotz, C., Martin, B.D.,

McDonald, D., McIver, L.J., Melnik, A.V., Metcalf, J.L., Morgan, S.C., Morton, J.T., Naimey, A.T., Navas-Molina, J.A., Nothias, L.F., Orchanian, S.B., Pearson, T., Peoples, S.L., Petras, D., Preuss, M.L., Pruesse, E., Rasmussen, L.B., Rivers, A., Robeson, M.S., Rosenthal, P., Segata, N., Shaffer, M., Shiffer, A., Sinha, R., Song, S.J., Spear, J.R., Swafford, A.D., Thompson, L.R., Torres, P.J., Trinh, P., Tripathi, A., Turnbaugh, P.J., Ul-Hasan, S., van der Hooft, J.J.J., Vargas, F., Vázquez-Baeza, Y., Vogtmann, E., von Hippel, M., Walters, W., Wan, Y., Wang, M., Warren, J., Weber, K. C., Williamson, C.H.D., Willis, A.D., Xu, Z.Z., Zaneveld, J.R., Zhang, Y., Zhu, Q., Knight, R., Caporaso, J.G., 2019. Reproducible, interactive, scalable and extensible microbiome data science using QIIME 2. Nat. Biotechnol. 37, 852–857. https://doi.org/10.1038/s41587-019-0209-9.

Brtnicky, M., Pecina, V., Galiova, M.V., Prokes, L., Zverina, O., Juricka, D., Klimanek, M., Kynicky, J., 2020. The impact of tourism on extremely visited volcanic island: link between environmental pollution and transportation modes. Chemosphere 249, 126118. https://doi.org/10.1016/j.chemosphere.2020.126118.

Burdige, D.J., 2007. Preservation of organic matter in marine sediments: controls, mechanisms, and an imbalance in sediment organic carbon budgets? Chem. Rev. 107, 467–485. https://doi.org/10.1021/cr050347q.

Chan, L.S., Ng, S.L., Davis, A.M., Yim, W.W.S., Yeung, C.H., 2001. Magnetic properties and heavy-metal contents of contaminated seabed sediments of Penny's Bay, Hong Kong. Mar. Pollut. Bull. 42, 569–583. https://doi.org/10.1016/S0025-326x(00)00203-4.

Chen, Z.Y., Saito, Y., Kanai, Y., Wei, T.Y., Li, L.Q., Yao, H.S., Wang, Z.H., 2004. Low concentration of heavy metals in the Yangtze estuarine sediments, China: a diluting setting. Estuar Coast Shelf S 60, 91–100. https://doi.org/10.1016/j.ecss.2003.11.021.

Chen, F., Lin, J., Qian, B., Wu, Z., Huang, P., Chen, K., Li, T., Cai, M., 2018. Geochemical assessment and spatial analysis of heavy metals in the surface sediments in the eastern Beibu gulf: a reflection on the industrial development of the South China Coast. IJERPH 15, 496. https://doi.org/10.3390/ijerph15030496.

Chen, Q., Lønborg, C., Chen, F., Gonsior, M., Li, Y., Cai, R., He, C., Chen, J., Wang, Y., Shi, Q., Jiao, N., Zheng, Q., 2022. Increased microbial and substrate complexity result in higher molecular diversity of the dissolved organic matter pool. Limnol. Oceanogr. 67, 2360–2373. https://doi.org/10.1002/lno.12206.

Chen, X., Cai, R., Zhuo, X., Chen, Q., He, C., Sun, J., Zhang, Y., Zheng, Q., Shi, Q., Jiao, N., 2023. Niche differentiation of microbial community shapes vertical distribution of recalcitrant dissolved organic matter in deep-sea sediments. Environ. Int. 178, 108080 https://doi.org/10.1016/j.envint.2023.108080.

Contursi, P., 2013. Responding to toxic compounds: a genomic and functional overview of Archaea. Front. Biosci. 18, 165. https://doi.org/10.2741/4094.

Coombs, J.M., Barkay, T., 2005. New findings on evolution of metal homeostasis genes: evidence from comparative genome analysis of bacteria and archaea. Appl. Environ. Microbiol. 71, 7083–7091. https://doi.org/10.1128/AEM.71.11.7083-7091.2005.

Cornall, A., Rose, A., Streten, C., McGuinness, K., Parry, D., Gibb, K., 2016. Molecular screening of microbial communities for candidate indicators of multiple metal impacts in marine sediments from northern Australia: microbial indicators of metal-impacted marine sediment. Environ. Toxicol. Chem. 35, 468–484. https://doi.org/10.1002/etc.3205.

Davis, T.A., Volesky, B., Mucci, A., 2003. A review of the biochemistry of heavy metal biosorption by brown algae. Water Res. 37, 4311–4330. https://doi.org/10.1016/S0043-1354(03)00293-8.

Dell'Anno, A., Mei, M.L., Ianni, C., Danovaro, R., 2003. Impact of bioavailable heavy metals on bacterial activities in coastal marine sediments. World J Microb Biot 19, 93–100. https://doi.org/10.1023/A:1022581632116.

Dell'Anno, F., Brunet, C., van Zyl, L.J., Trindade, M., Golyshin, P.N., Dell'Anno, A., Ianora, A., Sansone, C., 2020. Degradation of Hydrocarbons and Heavy Metal Reduction by Marine Bacteria in Highly Contaminated Sediments. Microorganisms 8. ARTN 1402. https://doi.org/10.3390/microorganisms8091402.

Dittmar, T., Koch, B., Hertkorn, N., Kattner, G., 2008. A simple and efficient method for the solid-phase extraction of dissolved organic matter (SPE-DOM) from seawater. Limnol Oceanogr-Meth 6, 230–235. https://doi.org/10.4319/lom.2008.6.230.

Dou, Y.G., Li, J., Zhao, J.T., Hu, B.Q., Yang, S.Y., 2013. Distribution, enrichment and source of heavy metals in surface sediments of the eastern Beibu Bay, South China Sea. Mar. Pollut. Bull. 67, 137–145. https://doi.org/10.1016/j.marpolbul.2012.11.022.

Ford, T., Sorci, J., Ika, R., Shine, J., 1998. Interactions between metals and microbial communities in New Bedford Harbor, Massachusetts. Environ Health Persp 106, 1033–1039. https://doi.org/10.2307/3434148.

Gan, H., Lin, J., Liang, K., Xia, Z., 2013. Selected trace metals (As, Cd and Hg) distribution and contamination in the coastal wetland sediment of the northern Beibu Gulf, South China Sea. Mar. Pollut. Bull. 66, 252–258. https://doi.org/10.1016/j.marpolbul.2012.09.020.

Gillan, D.C., Danis, B., Pernet, P., Joly, G., Dubois, P., 2005. Structure of sediment-associated microbial communities along a heavy-metal contamination gradient in the marine environment. Appl. Environ. Microbiol. 71, 679–690. https://doi.org/10.1128/Aem.71.2.679-690.2005.

Groeneveld, M., Catalán, N., Attermeyer, K., Hawkes, J., Einarsdóttir, K., Kothawala, D., Bergquist, J., Tranvik, L., 2020. Selective adsorption of terrestrial dissolved organic matter to inorganic surfaces along a boreal inland water continuum. JGR. Biogeosciences 125. https://doi.org/10.1029/2019JG005236 e2019JG005236.

Gu, Y.-G., Huang, H.-H., Liu, Y., Gong, X.-Y., Liao, X.-L., 2018. Non-metric multidimensional scaling and human risks of heavy metal concentrations in wild marine organisms from the Maowei Sea, the Beibu Gulf, South China Sea. Environ. Toxicol. Pharmacol. 59, 119–124. https://doi.org/10.1016/j.etap.2018.03.002.

Guo, W.D., Yang, L.Y., Zhai, W.D., Chen, W.Z., Osburn, C.L., Huang, X., Li, Y., 2014. Runoff-mediated seasonal oscillation in the dynamics of dissolved organic matter in different branches of a large bifurcated estuary—the Changjiang Estuary. J Geophys Res-Biogeo 119, 776–793. https://doi.org/10.1002/2013jg002540.

Hakanson, L., 1980. An ecological risk index for aquatic pollution-control - a sedimentological approach. Water Res. 14, 975–1001. https://doi.org/10.1016/0043-1354(80)90143-8.

He, C., Pan, Q., Li, P., Xie, W., He, D., Zhang, C., Shi, Q., 2019. Molecular Composition and Spatial Distribution of Dissolved Organic Matter (DOM) in the Pearl River Estuary. Environmental Chemistry, China. https://doi.org/10.1071/EN19051.

He, C., Zhang, Y., Li, Yunyun, Zhuo, X., Li, Yuguo, Zhang, C., Shi, Q., 2020. In-house standard method for molecular characterization of dissolved organic matter by FT-ICR mass spectrometry. ACS Omega. https://doi.org/10.1021/acsomega.0c01055.

Huang, H., Yuan, X., Zeng, G., Zhu, H., Li, H., Liu, Z., Jiang, H., Leng, L., Bi, W., 2011. Quantitative evaluation of heavy metals' pollution hazards in liquefaction residues of sewage sludge. Bioresour. Technol. 102, 10346–10351. https://doi.org/10.1016/j.biortech.2011.08.117.

Hyun, J.-H., Kim, B., Han, H., Baek, Y.-J., Lee, H., Cho, H., Yoon, S.-H., Kim, G., 2022. Sediment-derived dissolved organic matter stimulates heterotrophic prokaryotes metabolic activity in overlying deep sea in the Ulleung Basin. East Sea. Front. Mar. Sci. 9, 826592 https://doi.org/10.3389/fmars.2022.826592.

Jørgensen, L., Stedmon, C.A., Kragh, T., Markager, S., Middelboe, M., Søndergaard, M., 2011. Global trends in the fluorescence characteristics and distribution of marine dissolved organic matter. Mar. Chem. 126, 139–148. https://doi.org/10.1016/j.marchem.2011.05.002.

Kapili, B.J., Barnett, S.E., Buckley, D.H., Dekas, A.E., 2020. Evidence for phylogenetically and catabolically diverse active diazotrophs in deep-sea sediment. ISME J. 14, 971–983. https://doi.org/10.1038/s41396-019-0584-8.

Karimi, E., Keller-Costa, T., Slaby, B.M., Cox, C.J., Da Rocha, U.N., Hentschel, U., Costa, R., 2019. Genomic blueprints of sponge-prokaryote symbiosis are shared by low abundant and cultivatable Alphaproteobacteria. Sci. Rep. 9, 1999. https://doi.org/10.1038/s41598-019-38737-x.

Koho, K.A., Nierop, K.G.J., Moodley, L., Middelburg, J.J., Pozzato, L., Soetaert, K., van der Plicht, J., Reichart, G.J., 2013. Microbial bioavailability regulates organic matter preservation in marine sediments. Biogeosciences 10, 1131–1141. https://doi.org/10.5194/bg-10-1131-2013.

Kostka, J.E., Prakash, O., Overholt, W.A., Green, S.J., Freyer, G., Canion, A., Delgardio, J., Norton, N., Hazen, T.C., Huettel, M., 2011. Hydrocarbon-degrading bacteria and the bacterial community response in Gulf of Mexico Beach sands impacted by the Deepwater Horizon Oil Spill. Appl. Environ. Microbiol. 77, 7962–7974. https://doi.org/10.1128/AEM.05402-11.

Kothawala, D.N., Stedmon, C.A., Müller, R.A., Weyhenmeyer, G.A., Köhler, S.J., Tranvik, L.J., 2014. Controls of dissolved organic matter quality: evidence from a large-scale boreal lake survey. Glob. Chang. Biol. 20, 1101–1114. https://doi.org/10.1111/gcb.12488.

Lao, Q., Su, Q., Liu, G., Shen, Y., Chen, F., Lei, X., Qing, S., Wei, C., Zhang, C., Gao, J., 2019. Spatial distribution of and historical changes in heavy metals in the surface seawater and sediments of the Beibu Gulf, China. Mar. Pollut. Bull. 146, 427–434. https://doi.org/10.1016/j.marpolbul.2019.06.080.

Le, N.D., Hoang, T.T.H., Phung, V.P., Nguyen, T.L., Rochelle-Newall, E., Duong, T.T., Pham, T.M.H., Phung, T.X.B., Nguyen, T.D., Le, P.T., Pham, L.A., Nguyen, T.A.H., Le, T.P.Q., 2022. Evaluation of heavy metal contamination in the coastal aquaculture zone of the Red River Delta (Vietnam). Chemosphere 303, 134952. https://doi.org/10.1016/j.chemosphere.2022.134952.

Li, X., Meng, D., Li, J., Yin, H., Liu, H., Liu, X., Cheng, C., Xiao, Y., Liu, Z., Yan, M., 2017. Response of soil microbial communities and microbial interactions to long-term heavy metal contamination. Environ. Pollut. 231, 908–917. https://doi.org/10.1016/j.envpol.2017.08.057.

Li, Y., Tang, K., Zhang, L., Zhao, Z., Xie, X., Chen, C.-T.A., Wang, D., Jiao, N., Zhang, Y., 2018. Coupled carbon, sulfur, and nitrogen cycles mediated by microorganisms in the water column of a shallow-water hydrothermal ecosystem. Front. Microbiol. 9, 2718. https://doi.org/10.3389/fmicb.2018.02718.

Li, Y., Gong, X., Xiong, J., Sun, Y., Shu, Y., Niu, D., Lin, Y., Wu, L., Zhang, R., 2021. Different dissolved organic matters regulate the bioavailability of heavy metals and rhizosphere microbial activity in a plant-wetland soil system. J. Environ. Chem. Eng. 9, 106823 https://doi.org/10.1016/j.jece.2021.106823.

Liang, R.-Z., Gu, Y.-G., Li, H.-S., Han, Y.-J., Niu, J., Su, H., Jordan, R.W., Man, X.-T., Jiang, S.-J., 2023. Multi-index assessment of heavy metal contamination in surface sediments of the Pearl River estuary intertidal zone. Mar. Pollut. Bull. 186, 114445 https://doi.org/10.1016/j.marpolbul.2022.114445.

Lin, H., Guo, L., 2020. Variations in colloidal DOM composition with molecular weight within individual water samples as characterized by flow field-flow fractionation and EEM-PARAFAC analysis. Environ. Sci. Technol. 54, 1657–1667. https://doi.org/10.1021/acs.est.9b07123.

Lin, H., Lan, W., Feng, Q., Zhu, X., Li, T., Zhang, R., Song, H., Zhu, Y., Zhao, B., 2021. Pollution and ecological risk assessment, and source identification of heavy metals in sediment from the Beibu Gulf. South China Sea. Marine Pollution Bulletin 168, 112403. https://doi.org/10.1016/j.marpolbul.2021.112403.

Liu, S.H., Zeng, G.M., Niu, Q.Y., Liu, Y., Zhou, L., Jiang, L.H., Tan, X.F., Xu, P., Zhang, C., Cheng, M., 2017. Bioremediation mechanisms of combined pollution of PAHs and heavy metals by bacteria and fungi: a mini review. Bioresour. Technol. 224, 25–33. https://doi.org/10.1016/j.biortech.2016.11.095.

Liu, J., Cao, W., Jiang, H., Cui, J., Shi, C., Qiao, X., Zhao, J., Si, W., 2018. Impact of heavy metal pollution on ammonia oxidizers in soils in the vicinity of a Tailings Dam, Baotou, China. Bull. Environ. Contam. Toxicol. 101, 110–116. https://doi.org/10.1007/s00128-018-2345-1.

Liu, G.Q., Lao, Q.B., Su, Q.Z., Shen, Y.L., Chen, F.J., Qing, S.M., Wei, C.L., Zhang, C.H., 2020. Spatial and seasonal characteristics of dissolved heavy metals in the

aquaculture areas of Beibu Gulf, South China. Hum. Ecol. Risk. Assess. 26, 1957–1969. https://doi.org/10.1080/10807039.2019.1629273.
Long, Y., Jiang, J., Hu, X., Hu, J., Ren, C., Zhou, S., 2021. The response of microbial community structure and sediment properties to anthropogenic activities in Caohai wetland sediments. Ecotoxicol. Environ. Saf. 211, 111936 https://doi.org/10.1016/j.ecoenv.2021.111936.
Loring, D.H., Rantala, R.T.T., 1992. Manual for the geochemical analyses of marine sediments and suspended particulate matter. Earth Sci. Rev. 32, 235–283. https://doi.org/10.1016/0012-8252(92)90001-A.
Mahmoudi, N., Beaupre, S.R., Steen, A.D., Pearson, A., 2017. Sequential bioavailability of sedimentary organic matter to heterotrophic bacteria. Environ. Microbiol. 19, 2629–2644. https://doi.org/10.1111/1462-2920.13745.
Margesin, R., Płaza, G.A., Kasenbacher, S., 2011. Characterization of bacterial communities at heavy-metal-contaminated sites. Chemosphere 82, 1583–1588. https://doi.org/10.1016/j.chemosphere.2010.11.056.
Marshall, I.P.G., Starnawski, P., Cupit, C., Fernández Cáceres, E., Ettema, T.J.G., Schramm, A., Kjeldsen, K.U., 2017. The novel bacterial phylum Calditrichaeota is diverse, widespread and abundant in marine sediments and has the capacity to degrade detrital proteins: expansion of Calditrichaeota diversity. Environ. Microbiol. Rep. 9, 397–403. https://doi.org/10.1111/1758-2229.12544.
Meng, J., Xu, J., Qin, D., He, Y., Xiao, X., Wang, F., 2014. Genetic and functional properties of uncultivated MCG archaea assessed by metagenome and gene expression analyses. ISME J. 8, 650–659. https://doi.org/10.1038/ismej.2013.174.
Moreira, V.A., Cravo-Laureau, C., De Carvalho, A.C.B., Baldy, A., Bidone, E.D., Sabadini-Santos, E., Duran, R., 2023. Microbial indicators along a metallic contamination gradient in tropical coastal sediments. J. Hazard. Mater. 443, 130244 https://doi.org/10.1016/j.jhazmat.2022.130244.
Nogales, B., Aguiló-Ferretjans, M.M., Martín-Cardona, C., Lalucat, J., Bosch, R., 2007. Bacterial diversity, composition and dynamics in and around recreational coastal areas. Environ. Microbiol. 9, 1913–1929. https://doi.org/10.1111/j.1462-2920.2007.01308.x.
Parkes, J.R., Cragg, B., Roussel, E., Webster, G., Weightman, A., Sass, H., 2014. A review of prokaryotic populations and processes in sub-seafloor sediments, including biosphere: geosphere interactions. Mar. Geol. 352, 409–425. https://doi.org/10.1016/j.margeo.2014.02.009.
Petrie, L., North, N.N., Dollhopf, S.L., Balkwill, D.L., Kostka, J.E., 2003. Enumeration and characterization of iron(III)-reducing microbial communities from acidic subsurface sediments contaminated with uranium (VI). Appl. Environ. Microbiol. 69, 7467–7479. https://doi.org/10.1128/AEM.69.12.7467-7479.2003.
Pontoni, L., La Vecchia, C., Boguta, P., Sirakov, M., D'Aniello, E., Fabbricino, M., Locascio, A., 2022. Natural organic matter controls metal speciation and toxicity for marine organisms: a review. Environ. Chem. Lett. 20, 797–812. https://doi.org/10.1007/s10311-021-01310-y.
Rajeev, M., Sushmitha, T.J., Aravindraja, C., Toleti, S.R., Pandian, S.K., 2021. Exploring the impacts of heavy metals on spatial variations of sediment-associated bacterial communities. Ecotox Environ Safe 209, 111808. https://doi.org/10.1016/j.ecoenv.2020.111808.
Ren, Y., Niu, J., Huang, W., Peng, D., Xiao, Y., Zhang, X., Liang, Y., Liu, X., Yin, H., 2016. Comparison of microbial taxonomic and functional shift pattern along contamination gradient. BMC Microbiol. 16, 110. https://doi.org/10.1186/s12866-016-0731-6.
Roth, V.-N., Lange, M., Simon, C., Hertkorn, N., Bucher, S., Goodall, T., Griffiths, R.I., Mellado-Vázquez, P.G., Mommer, L., Oram, N.J., Weigelt, A., Dittmar, T., Gleixner, G., 2019. Persistence of dissolved organic matter explained by molecular changes during its passage through soil. Nat. Geosci. 12, 755–761. https://doi.org/10.1038/s41561-019-0417-4.
Saw, J.H.W., Nunoura, T., Hirai, M., Takaki, Y., Parsons, R., Michelsen, M., Longnecker, K., Kujawinski, E.B., Stepanauskas, R., Landry, Z., Carlson, C.A., Giovannoni, S.J., 2020. Pangenomics Analysis Reveals Diversification of Enzyme Families and Niche Specialization in Globally Abundant SAR202 Bacteria, mBio 11. https://doi.org/10.1128/mBio.02975-19 e02975-19.
Sazykin, I., Khmelevtsova, L., Azhogina, T., Sazykina, M., 2023. Heavy metals influence on the bacterial community of soils: a review. Agriculture 13, 653. https://doi.org/10.3390/agriculture13030653.
Segata, N., Izard, J., Waldron, L., Gevers, D., Miropolsky, L., Garrett, W.S., Huttenhower, C., 2011. Metagenomic biomarker discovery and explanation. Genome Biol. 12, R60. https://doi.org/10.1186/gb-2011-12-6-r60.
Sepehri, A., Sarrafzadeh, M.-H., 2018. Effect of nitrifiers community on fouling mitigation and nitrification efficiency in a membrane bioreactor. Chemical Engineering and Processing - Process Intensification 128, 10–18. https://doi.org/10.1016/j.cep.2018.04.006.
Sepehri, A., Sarrafzadeh, M.-H., Avateffazeli, M., 2020. Interaction between Chlorella vulgaris and nitrifying-enriched activated sludge in the treatment of wastewater with low C/N ratio. J. Clean. Prod. 247, 119164 https://doi.org/10.1016/j.jclepro.2019.119164.
Shi, G., Chen, Z., Bi, C., Li, Y., Teng, J., Wang, L., Xu, S., 2010. Comprehensive assessment of toxic metals in urban and suburban street deposited sediments (SDSs) in the biggest metropolitan area of China. Environ. Pollut. 158, 694–703. https://doi.org/10.1016/j.envpol.2009.10.020.
Song, B., Zhang, C., Zeng, G.M., Gong, J.L., Chang, Y.N., Jiang, Y., 2016. Antibacterial properties and mechanism of graphene oxide-silver nanocomposites as bactericidal agents for water disinfection. Arch. Biochem. Biophys. 604, 167–176. https://doi.org/10.1016/j.abb.2016.04.018.
Stedmon, C.A., Bro, R., 2008. Characterizing dissolved organic matter fluorescence with parallel factor analysis: a tutorial. Limnol Oceanogr-Meth 6, 572–579. https://doi.org/10.4319/lom.2008.6.572.
Subrahmanyam, G., Hu, H.-W., Zheng, Y.-M., Gattupalli, A., He, J.-Z., Liu, Y.-R., 2014. Response of ammonia oxidizing microbes to the stresses of arsenic and copper in two acidic alfisols. Appl. Soil Ecol. 77, 59–67. https://doi.org/10.1016/j.apsoil.2014.01.011.
Sun, Y., Zhou, Q., Xie, X., Liu, R., 2010. Spatial, sources and risk assessment of heavy metal contamination of urban soils in typical regions of Shenyang, China. J. Hazard. Mater. 174, 455–462. https://doi.org/10.1016/j.jhazmat.2009.09.074.
Superville, P.J., Prygiel, E., Magnier, A., Lesven, L., Gao, Y., Baeyens, W., Ouddane, B., Dumoulin, D., Billon, G., 2014. Daily variations of Zn and Pb concentrations in the Defile River in relation to the resuspension of heavily polluted sediments. Sci. Total Environ. 470, 600–607. https://doi.org/10.1016/j.scitotenv.2013.10.015.
Tang, J.Y., Zhang, J.C., Ren, L.H., Zhou, Y.Y., Gao, J., Luo, L., Yang, Y., Peng, Q.H., Huang, H.L., Chen, A.W., 2019. Diagnosis of soil contamination using microbiological indices: a review on heavy metal pollution. J. Environ. Manage. 242, 121–130. https://doi.org/10.1016/j.jenvman.2019.04.061.
Tang, G., Zheng, X., Li, B., Chen, S., Zhang, B., Hu, S., Qiao, H., Liu, T., Wang, Q., 2022. Trace metal complexation with dissolved organic matter stresses microbial metabolisms and triggers community shifts: the intercorrelations. Environ. Pollut. 314, 120221 https://doi.org/10.1016/j.envpol.2022.120221.
Tangherlini, M., Corinaldesi, C., Rastelli, E., Musco, L., Armiento, G., Danovaro, R., Dell'Anno, A., 2020. Chemical contamination can promote turnover diversity of benthic prokaryotic assemblages: the case study of the Bagnoli-Coroglio bay (southern Tyrrhenian Sea). Mar. Environ. Res. 160, 105040 https://doi.org/10.1016/j.marenvres.2020.105040.
Tipayno, S.C., Truu, J., Samaddar, S., Truu, M., Preem, J.-K., Oopkaup, K., Espenberg, M., Chatterjee, P., Kang, Y., Kim, K., Sa, T., 2018. The bacterial community structure and functional profile in the heavy metal contaminated paddy soils, surrounding a nonferrous smelter in South Korea. Ecol. Evol. 8, 6157–6168. https://doi.org/10.1002/ece3.4170.
Volant, A., Desoeuvre, A., Casiot, C., Lauga, B., Delpoux, S., Morin, G., Personné, J.C., Héry, M., Elbaz-Poulichet, F., Bertin, P.N., Bruneel, O., 2012. Archaeal diversity: temporal variation in the arsenic-rich creek sediments of Carnoulès Mine, France. Extremophiles 16, 645–657. https://doi.org/10.1007/s00792-012-0466-8.
Wang, Y.Q., Yang, L.Y., Kong, L.H., Liu, E.F., Wang, L.F., Zhu, J.R., 2015. Spatial distribution, ecological risk assessment and source identification for heavy metals in surface sediments from Dongping Lake, Shandong, East China. Catena 125, 200–205. https://doi.org/10.1016/j.catena.2014.10.023.
Wang, C., Guo, W.D., Li, Y., Stubbins, A., Li, Y.Z., Song, G.D., Wang, L., Cheng, Y.Y., 2017. Hydrological and biogeochemical controls on absorption and fluorescence of dissolved organic matter in the Northern South China Sea. J Geophys Res-Biogeo 122, 3405–3418. https://doi.org/10.1002/2017jg004100.
Wang, Linqiong, Li, Y., Niu, L., Zhang, W., Zhang, H., Wang, Longfei, Wang, P., 2018. Response of ammonia oxidizing archaea and bacteria to decabromodiphenyl ether and copper contamination in river sediments. Chemosphere 191, 858–867. https://doi.org/10.1016/j.chemosphere.2017.10.067.
Wang, W., Tao, J., Yu, K., He, C., Wang, J., Li, P., Chen, H., Xu, B., Shi, Q., Zhang, C., 2021a. Vertical Stratification of Dissolved Organic Matter Linked to Distinct Microbial Communities in Subtropic Estuarine Sediments. Front. Microbiol. 12, 697860 https://doi.org/10.3389/fmicb.2021.697860.
Wang, C., Wang, Y., Liu, P., Sun, Y., Song, Z., Hu, X., 2021b. Characteristics of bacterial community structure and function associated with nutrients and heavy metals in coastal aquaculture area. Environ. Pollut. 275, 116639 https://doi.org/10.1016/j.envpol.2021.116639.
Wang, Y., Xie, R., Shen, Y., Cai, R., He, C., Chen, Q., Guo, W., Shi, Q., Jiao, N., Zheng, Q., 2022. Linking microbial population succession and DOM molecular changes in *Synechococcus* -derived organic matter addition incubation. Microbiol Spectr. https://doi.org/10.1128/spectrum.02308-21 e02308-21.
Weishaar, J.L., Aiken, G.R., Bergamaschi, B.A., Fram, M.S., Fujii, R., Mopper, K., 2003. Evaluation of specific ultraviolet absorbance as an Indicator of the chemical composition and reactivity of dissolved organic carbon. Environ. Sci. Technol. 37, 4702–4708. https://doi.org/10.1021/es030360x.
Wu, Z., Xu, Y., Cai, M.G., Cheng, S.Y., Chen, H.R., Huang, D.R., Chen, K., Lin, Y., Li, T.Y., Liu, M.Y., Deng, H.X., Ni, M.J., Ke, H.W., 2017. Metals in fishes from Yongshu Island, Southern South China Sea: human health risk assessment. J Toxicol-Us 2017, 2458293. https://doi.org/10.1155/2017/2458293.
Xia, P., Meng, X.W., Yin, P., Cao, Z.M., Wang, X.Q., 2011. Eighty-year sedimentary record of heavy metal inputs in the intertidal sediments from the Nanliu River estuary, Beibu Gulf of South China Sea. Environ. Pollut. 159, 92–99. https://doi.org/10.1016/j.envpol.2010.09.014.
Xiao, H., Shahab, A., Ye, F., Wei, G., Li, J., Deng, L., 2022a. Source-specific ecological risk assessment and quantitative source apportionment of heavy metals in surface sediments of Pearl River Estuary. China. Marine Pollution Bulletin 179, 113726. https://doi.org/10.1016/j.marpolbul.2022.113726.
Xiao, H., Shahab, A., Ye, F., Wei, G., Li, J., Deng, L., 2022b. Source-specific ecological risk assessment and quantitative source apportionment of heavy metals in surface sediments of Pearl River Estuary. China. Marine Pollution Bulletin 179, 113726. https://doi.org/10.1016/j.marpolbul.2022.113726.
Xu, D., Wang, R., Wang, W., Ge, Q., Zhang, W., Chen, L., Chu, F., 2019. Tracing the source of Pb using stable Pb isotope ratios in sediments of eastern Beibu Gulf, South China Sea. Mar. Pollut. Bull. 141, 127–136. https://doi.org/10.1016/j.marpolbul.2019.02.028.
Xu, J., Chen, Q., Lønborg, C., Li, Y., Cai, R., He, C., Shi, Q., Hu, Y., Wang, Y., Jiao, N., Zheng, Q., 2022. You exude what you eat: how carbon-, nitrogen-, and sulfur-rich organic substrates shape microbial community composition and the dissolved organic matter pool. Appl. Environ. Microbiol. 88, e01558-22 https://doi.org/10.1128/aem.01558-22.

Yang, Y., Li, Y., Sun, Q., 2014. Archaeal and bacterial communities in acid mine drainage from metal-rich abandoned tailing ponds, Tongling, China. Trans. Nonferrous Met. Soc. Chin. 24, 3332–3342. https://doi.org/10.1016/S1003-6326(14)63474-9.

Yu, R.L., Yuan, X., Zhao, Y.H., Hu, G.R., Tu, X.L., 2008. Heavy metal pollution in intertidal sediments from Quanzhou Bay, China. J. Environ. Sci. 20, 664–669. https://doi.org/10.1016/S1001-0742(08)62110-5.

Yu, T., Wu, W., Liang, W., Lever, M.A., Hinrichs, K.-U., Wang, F., 2018. Growth of sedimentary *Bathyarchaeota* on lignin as an energy source. Proc. Natl. Acad. Sci. U. S. A. 115, 6022–6027. https://doi.org/10.1073/pnas.1718854115.

Yu, T., Hu, H., Zeng, X., Wang, Y., Pan, D., Deng, L., Liang, L., Hou, J., Wang, F., 2023. Widespread Bathyarchaeia encode a novel methyltransferase utilizing lignin-derived aromatics. mLife 2, 272–282. https://doi.org/10.1002/mlf2.12082.

Zanaroli, G., Negroni, A., Vignola, M., Nuzzo, A., Shu, H., Fava, F., 2012. Enhancement of microbial reductive dechlorination of polychlorinated biphenyls (PCBs) in a marine sediment by nanoscale zerovalent iron (NZVI) particles. J. Chemical Tech & Biotech 87, 1246–1253. https://doi.org/10.1002/jctb.3835.

Zeng, X.-Y., Li, S.-W., Leng, Y., Kang, X.-H., 2020. Structural and functional responses of bacterial and fungal communities to multiple heavy metal exposure in arid loess. Sci. Total Environ. 723, 138081 https://doi.org/10.1016/j.scitotenv.2020.138081.

Zeng, T., Wang, L., Zhang, X., Song, X., Li, J., Yang, J., Chen, S., Zhang, J., 2022. Characterization of microbial communities in wastewater treatment plants containing heavy metals located in chemical industrial zones. IJERPH 19, 6529. https://doi.org/10.3390/ijerph19116529.

Zeng, K., Huang, X., Dai, C., He, C., Chen, H., Guo, J., Xin, G., 2024. Bacterial community regulation of soil organic matter molecular structure in heavy metal-rich mangrove sediments. J. Hazard. Mater. 465, 133086 https://doi.org/10.1016/j.jhazmat.2023.133086.

Zhang, Z.-F., Pan, J., Pan, Y.-P., Li, M., 2021a. Biogeography, assembly patterns, driving factors, and interactions of archaeal community in mangrove sediments. mSystems 6, e01381-20. https://doi.org/10.1128/mSystems.01381-20.

Zhang, J., Shi, Q., Fan, S., Zhang, Y., Zhang, M., Zhang, Jianfeng, 2021b. Distinction between Cr and other heavy–metal–resistant bacteria involved in C/N cycling in contaminated soils of copper producing sites. J. Hazard. Mater. 402, 123454 https://doi.org/10.1016/j.jhazmat.2020.123454.

Zhao, B., Wang, X., Jin, H., Feng, H., Shen, G., Cao, Y., Yu, C., Lu, Z., Zhang, Q., 2018a. Spatiotemporal variation and potential risks of seven heavy metals in seawater, sediment, and seafood in Xiangshan Bay, China (2011–2016). Chemosphere 212, 1163–1171. https://doi.org/10.1016/j.chemosphere.2018.09.020.

Zhao, G., Ye, S., Yuan, H., Ding, X., Wang, J., Laws, E.A., 2018b. Surface sediment properties and heavy metal contamination assessment in river sediments of the Pearl River Delta, China. Mar. Pollut. Bull. 136, 300–308. https://doi.org/10.1016/j.marpolbul.2018.09.035.

Zhao, Z., Li, H., Sun, Y., Zhan, A., Lan, W., Woo, S.P., Shau-Hwai, A.T., Fan, J., 2022. Bacteria versus fungi for predicting anthropogenic pollution in subtropical coastal sediments: assembly process and environmental response. Ecol. Indic. 134, 108484 https://doi.org/10.1016/j.ecolind.2021.108484.

Zheng, N., Wang, Q.C., Liang, Z.Z., Zheng, D.M., 2008. Characterization of heavy metal concentrations in the sediments of three freshwater rivers in Huludao City, Northeast China. Environ. Pollut. 154, 135–142. https://doi.org/10.1016/j.envpol.2008.01.001.

Zhou, Z., Pan, J., Wang, F., Gu, J.-D., Li, M., 2018. Bathyarchaeota: globally distributed metabolic generalists in anoxic environments. FEMS Microbiol. Rev. 42, 639–655. https://doi.org/10.1093/femsre/fuy023.